

# Precursor Identification and Physical Mechanism of Fiber-Form Nanostructure Growth on Metal Surfaces with Helium Plasma Irradiation

ヘリウムプラズマ照射を受けた金属表面に成長する  
纖維状ナノ構造形成の先駆体の同定と物理成長過程

Shuichi TAKAMURA<sup>†</sup>, Yoshihiko UESUGI<sup>† †</sup>  
高村 秀一, 上杉 喜彦

**Abstract** The initial stage of fiber-form nanostructure growth on metal surfaces with helium plasma irradiation is investigated with FE-SEM images by a technique that allows time evolution of nanostructure growth converted to spatial variation. It is concluded that loop-like nano-scale structure are thought to be precursors of fiber-form tendrils. Loop fractures and branching out are considered as possible candidates of the nano-fiber growth. Each schematic sketch for the above initial stages is given. Growth mechanism of fibers is discussed in terms of shear modulus of materials.

## 1. Introduction

Since the discovery of fiber-form nanostructure on tungsten (W) surfaces irradiated by helium plasmas<sup>1), 2)</sup>, a lot of attentions have been paid from many kinds of aspects<sup>3)</sup>. The reason why such structures may be formed has been very interested experimentally<sup>4)</sup>, theoretically<sup>5), 6)</sup> and from numerical simulations<sup>7), 8)</sup> over the world, from the viewpoints of not only plasma-wall interactions in fusion devices<sup>9)</sup> but also fundamental physics and industrial applications. The temperature range for formation of W nanostructure is 1000 ~ 2000 K. However, the uppermost temperature may change under a competition of formation and annihilation of nanostructure so that it depends on ion flux density. Molybdenum (Mo) needs the temperature range, 800 ~ 1050 K<sup>10)</sup>. The surface morphology is very

similar to that of W. But the Mo fibers have about twice as thick as those of W. On the other hand, tantalum (Ta) having the same bcc crystal structure as W and Mo does not show any fiber-form structure in a wide temperature range, (0.2 ~ 0.4) T<sub>m</sub><sup>11)</sup> and at further lower temperature where T<sub>m</sub> = 3290 K is the melting point although the bubbles and holes are formed at relatively high temperature. Ta has relatively low viscosity or shear modulus among refractory metals. As shown by Krasheninnikov theory<sup>5)</sup> and MD simulation of Smirnov<sup>6)</sup>, the formation mechanism seems to be deeply related to an appropriate viscous character of metals with helium nano-bubbles or clusters and a viscoelastic fluid motion over some finite temperature band.

On the other hand, fiber-form nanostructure is annihilated out and recovered to almost flat original surface at high temperature without any energetic helium ion irradiation although nano-size bubbles remain about 100 nm underneath the recovered

† Faculty of Engineering, AIT, Toyota 470-0392

† † Institute of Science and Engineering, Kanazawa University, Kanazawa 920-1192

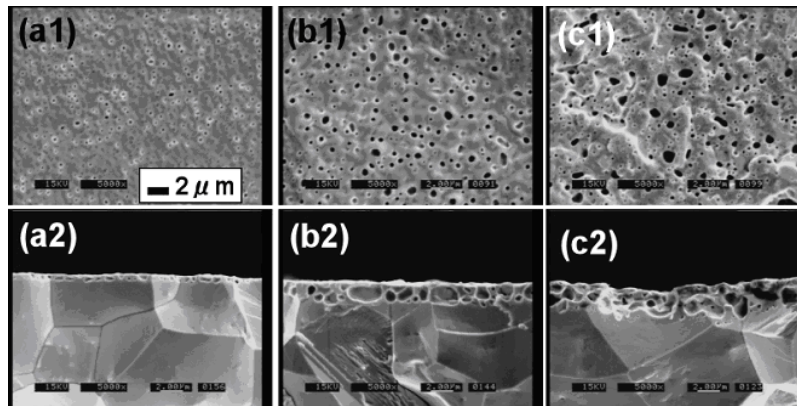


Fig.1 Surface defect development of high temperature PM-W (Powder Metallurgy - tungsten) tungsten irradiated by high helium ion flux. The surface temperature is 2200 K, the ion energy is 15 eV and the ion flux is  $8.3 \times 10^{22} \text{ m}^{-2} \text{ s}^{-1}$ . Irradiation time is (a) 1000 s, (b) 10000 s and (c) 750000 s. (a-1) ~ (c-1) show top views while (a-2) ~ (c-2) do cross-sections observed with SEM.

surface<sup>12)</sup>. However, Elastic Recoil Detection (ERD) using oxygen ion beam reveals too small He atomic concentration imbedded in W nano-fibers<sup>13)</sup>, compared with the prediction from viscoelastic model.

As shown above, physical mechanism of fiber-form nanostructure formation on metal surfaces is not conclusive so far. Therefore, the present research proposes a model on initial formation process from experimental stand points, using a flux gradient method, and, some discussions are given on a relation to physical properties of several metals.

## 2. Experimental Procedure

Main plasma generation machine is AIT-PID (Aichi Institute of Technology – Plasma Irradiation Device)<sup>14)</sup>. Helium plasma density has of order of  $10^{18} \text{ m}^{-3}$ , electron temperature of bulk component is about 5 eV and its high energy component has an effective temperature of about 30 eV. High energy electron component has about 10 % of total electron population. The ion flux to metal specimen has more than  $10^{21} \text{ m}^{-2} \text{ s}^{-1}$ .

Capability of standard SEM is not sufficient to look at fiber-form structure so that it was observed as “fuzz”. FE-SEM (Field Emission – Scanning Electron Microscope) has a sufficient capability to observe fiber-form nanostructure. In the present research an

innovative technique for initial formation process, conversion of temporal growth process to spatial variation, that is, a technique employing a spatial gradient of He ion flux on metal surface.

Concerning surface temperature measurement, we may employ radiation thermometer with the knowledge of spectral emissivity which is specific to target material and morphology. We may know spectral emissivity of non-damaged virgin metal surface<sup>15)</sup>. But we do not know precisely the emissivity of He defected tungsten, for example. Moreover, well-grown fiber-form nanostructure has an emissivity of almost black body. On the other hand, R or K type thermocouple with thin insulated sheath is also effective for surface damaged metals.

## 3. Experimental Observations

### 3.1 Nanostructure Formation on Tungsten Surfaces

Historically, bubbles and holes on tungsten surface observed with SEM level are found 18 years before as one of helium defects<sup>16)</sup>. Figure 1 shows surface defect development at high temperature, say more than 2000 K, with high He ion flux. But it has been said that the temperature for bubbles and holes formation would be too high on divertor target plate in fusion devices. However, it could be the case at transient thermal events, like ELMs and vertical displacement events in

Precursor Identification and Physical Mechanism of Fiber-Form Nanostructure Growth on  
Metal Surfaces with Helium Plasma Irradiation

ITER (International Thermonuclear Experimental Reactor), moreover at a steady state in fusion power reactor. Experimentally, the lower limit of incident He ion energy for the above defects was found to be about 6 eV by adjusting the potential difference between W target and plasma potential<sup>17)</sup>. The value of surface potential barrier has been confirmed theoretically<sup>18)</sup> and numerically<sup>19)</sup>. Anyway, identification trial of lowest temperature limit for bubble and hole formation leads us to a finding of fiber-form nanostructure<sup>1)</sup>. The lowest ion incident energy was found to be about 25 eV<sup>20)</sup> probably because of a need of sufficient range of incident He ions.

As described in the first section, viscous property like a starch syrup seems to us an essential feature for the growth of nano-fibers containing He nano-bubbles of clusters so that Krasheninnikov proposed a viscoelastic model<sup>5)</sup>. However, He content in nano-fibers predicted by the above model does not explain its experimental evaluation. On the other hand, Martynenko et al. presented a growth model due to accumulation of He adatoms on fiber tips where the adatoms tend not to be movable. Moreover, they claim that threshold He ion energy for growth and growth speed regulated by a diffusive process may be explained by their model. But there is no explanation of He bubbles and unique feature of He ions.

Therefore, comprehensive modeling or theory is not available at the moment so that we have to come back to the detailed experimental observations on the time evolution of fiber-form nanostructure growth.

We have been developing a special technique, a conversion from temporal development of nanostructure growth to spatial variation with a single He plasma exposure of metal surface, associated by FE-SEM observation. We call this technique “flux gradient method”. W nano-walls with hole and standing arch or loop are identified to be a precursor for growth of fiber-form nanostructure<sup>21)</sup>. Molybdenum has a similar behavior.

Well-developed fiber-form nanostructures are shown in Fig.2 where (a) shows fuzzy structure developed on both sides of thin W foil with the original thickness of 3

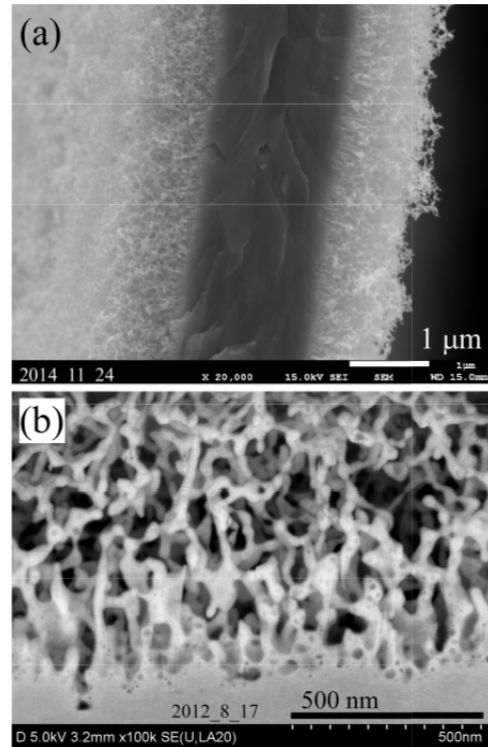


Fig.2 Typical FE-SEM images of fiber-form nanostructure formed on PM-W surfaces. (a) Fractured cross-section of tungsten foil with the original thickness of 3 μm. Growth of fiber-form nanostructure on both sides brings the apparent thickness of about 4 μm. (b) Oblique view of cross-section of nanostructured tungsten obtained by CP method with a large magnification. Nano-bubbles inside nano-fibers can be distinguished.

μm, and (b) shows a grazing view of cross-section obtained with CP (Cross-sectional Polishing) method, where we can see that arborescent nano-fibers contain many nano-bubbles. Moreover, we note that holes on the surfaces of nano-fibers are distinguished. These holes show bursting of He gas from nano-bubbles in nano-fibers. In Fig.2(a) the final thickness becomes approximately 4 μm, thicker than the original foil thickness. Macroscopically, a complete black color was obtained. Detailed evaluation shows not only some spectral emissivities which appear at Planck's radiation formula but also total emissivity which is contained in Stefan-Boltzmann law becomes about unity<sup>22)</sup>.

Figure 3 shows the procedure for flux-gradient method (a) and FE-SEN images of a fractured cross-section of a W sample (b, c). Half of a rectangular W surface with a thickness of 35 μm was covered with

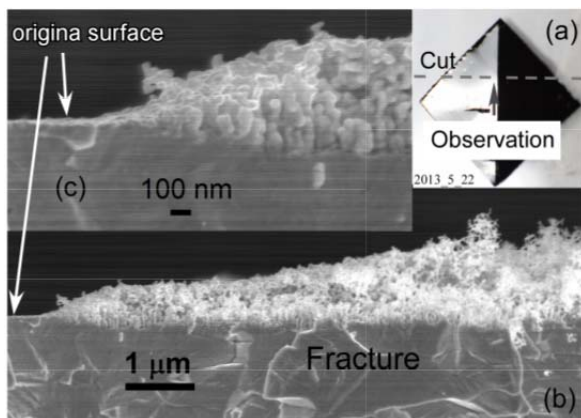


Fig.3 Fractured cross-section of the boundary zone the virgin through the damaged surface. (a) Photo showing the macroscopic boundary zone and fractured dotted line, (b) and (c) are FE-SEM images. Helium ion flux on the uncovered area is  $3.8 \times 10^{21} \text{ m}^{-2} \cdot \text{s}^{-1}$ , and its fluence is  $2.7 \times 10^{25} \text{ m}^{-2}$  with the ion energy of 105 eV, and an initial tungsten temperature of 1300 K.

a thin (15 μm) W foil. After a He plasma exposure, the thin cover foil was removed from the main W sheet, as shown in Fig.3(a). Crossing a boundary between the original surface and the He affected area, a fractured cross-section was obtained along the broken line. Macroscopically, the boundary seems to be sharp, but that is not the case microscopically, as shown in Fig.3(b). The incident ion flux has a gradient, which in turn causes the ion fluence on W surface to have a gradient. This allows a temporal evolution of the nanostructure growth to be converted to a spatial variation. A detailed view is shown in Fig.3(c), indicating clearly that the nanostructure formation is started by pitting the original surface, arising from the arrival of bubbles to the surface due to thermal motion of He bubbles<sup>23)</sup> and a bursting of He gas<sup>19)</sup>. The pitting is about 200 nm in depth in the present case, while the tip of the defect has a diameter of ~ 100 nm initially, growing as nano-fibers with the final diameter of a few tens nanometers.

Figure 4(a) shows a top view of the above mentioned boundary zone. Dark areas suggest holes generated by bubble migration to the surface from the interior of material bulk<sup>21)</sup>. In the right-most region, many protrusion appear, growing as fibers. In order to clearly

demonstrate an increase in hole area, binarization from gray to black or white was performed for three different zones (i) ~ (ii), where each zone has 8.0 μm in vertical range and 2.0 μm in width and (i) is close to the originally unexposed surface, (iii) containing W nano-fibers and (ii) is located between (i) and (iii). Black areas may represent not only real holes on the surface, but also holes of loops or arches. The area occupied by “holes” is 16 %, 42 % and 60 % for (i), (ii) and (iii), respectively. The mean hole diameter is 40 nm, 56 nm and 200 nm, respectively.

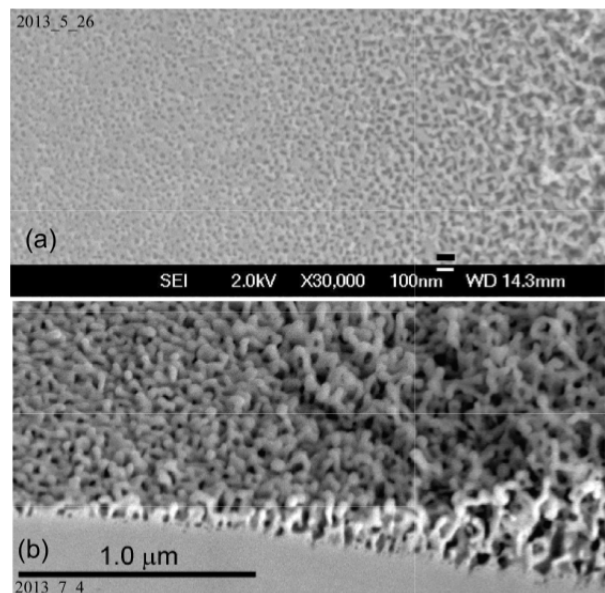


Fig.4 (a) Top view of the tungsten boundary zone. (b) Oblique view of cross-section of boundary zone obtained with CP method, showing many loop-like structures.

From this estimation, it is assumed that the remaining surface area without holes becomes thin and fine-grained. Those structural changes may serve as a background for the formation of loops or arches as precursors for the fiber-form nanostructure growth mentioned below. The FE-SEM images obtained with similar experimental parameters to those in Figs.2 and 3 correspond to a grazing view of the cross-section made with the CP (Cross-section Polishing) method using an argon ion beam, as shown in Fig.4(b), over the boundary zone between the low ion fluence (left side) and the high one (right side).

Many loop or arch like structures are already observed in the left side of Fig.4(b) whereas

Precursor Identification and Physical Mechanism of Fiber-Form Nanostructure Growth on Metal Surfaces with Helium Plasma Irradiation

well-developed nano-fibers are seen in the right region. It seems that some loops stand almost perpendicular to the original surface, but others are at different angles, and the orientation of the loop surface is random. However, the size of loops is somewhat coherent. In the low-fluence region, the outer diameter of the loops is ~ 70 nm and the inner one is ~ 30 nm, while in the high fluence region close to the nano-fiber growth area, the diameters become 150 nm and 70 nm, respectively.

As shown in the right half of Fig.4(b), loop or arch like structure grow in size and becomes nano-fibers by branching-out or fracturing as if W nano-fibers containing He nano-bubbles behaves as viscoelastic fluid. Such viscous fluid-like behavior can be seen on the way of annealing process which annihilates fiber-form structure as shown in Fig.5, where (a)

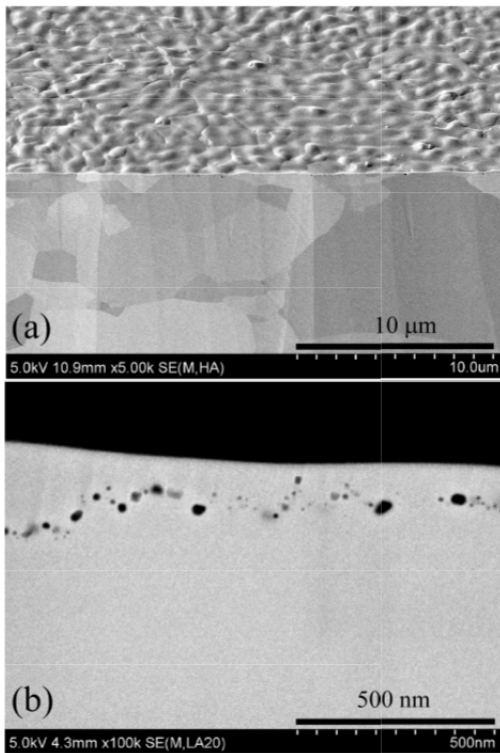


Fig.5 Surface morphology of PM-W tungsten recovered by 60 min helium plasma irradiation with almost constant surface temperature of 1800 K. The ion incident energy is approximately 4 ~ 5 eV, well below the threshold energy of 25 eV. (a) a grazing view of the cross-section obtained with CP method, showing a melting of nano-fibers something like a heated starch syrup. (b) magnified view of the cross-section showing tiny helium bubbles 100 nm underneath the surface.

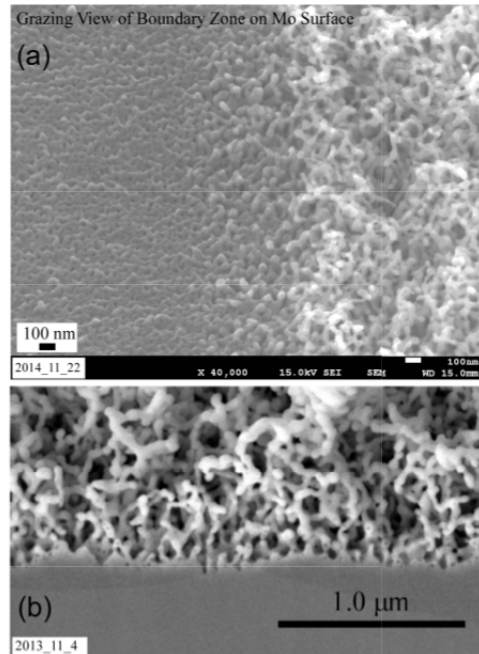


Fig.6 Molybdenum fuzz formation. (a) Grazing view of boundary zone on Mo surface obtained with flux gradient method, and (b) oblique view of cross-section of well-developed Mo fuzz.

corresponds to a grazing view of recovered rather flat surface and (b) shows the cross-section near the surface, indicating a series of tiny bubbles with diameters less than 100 nm about 100 nm beneath the surface<sup>12)</sup>. These annealing processes also reproduce a starch syrup property.

### 3.2 Nanostructure Formation on Surfaces of Other Metals

Observations similar to W were obtained firstly for Mo surface irradiated by He plasmas, as shown in Fig.6, (a) of which is an FE-SEM images of the boundary zone looked obliquely, obtained with the flux-gradient method. We can reconfirm the presence of the loop or arch like nanostructure development, the size of which is roughly twice as large as those of W<sup>10)</sup>. The nano-fibers themselves have diameter again about twice as thick as those of W. Figure 6(b) shows other SEM photos of a cross-section obtained with CP method, where fiber-form nanostructure is well developed.

Secondly, helium-defected nickel (Ni) surface produced with flux gradient method was observed with

FE-SEM, as shown in Fig.7 where (a) is the photo of virgin Ni target mounted on a cooled stage, (b) is the Ni target after He plasma irradiation at the temperature of 680 K in which boundary zones are created by shadows of washers for fixing the target on the stage, and (c) is a top view of boundary zone with FE-SEM in which the He flux increases from left to right. Here we can also distinguish a development of loop-like structure. However, morphology of well-developed nanostructure for Ni is not entangled fibers but an ensemble of straight fibers and/or thin nano-walls.

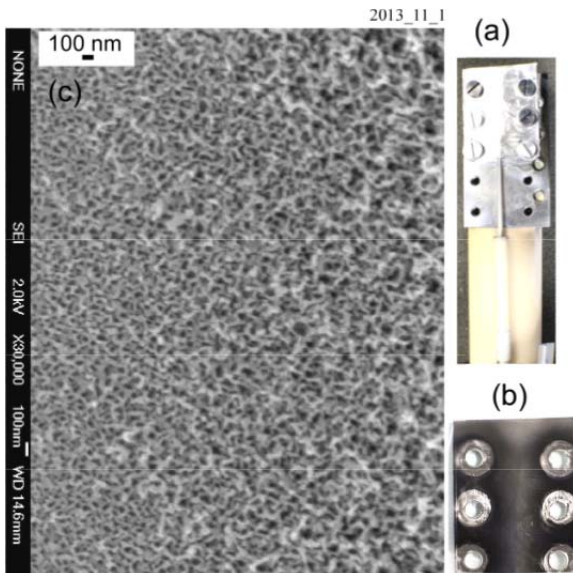


Fig.7 Helium defect of nickel sheet ( $24 \times 30 \times 0.1 \text{ mm}^3$ ). (a) Installation of nickel specimen on a cooled stainless-steel stage, (b) photo of nickel specimen after helium plasma exposure (Temperature is about 680 K measured with K-type thermocouple, ion bombarding energy is 55 eV and the ion flux is  $6 \times 10^{21} \text{ m}^{-2} \cdot \text{s}^{-1}$ ), and (c) FE-SEM image of boundary zone between hidden virgin area and helium irradiated black region.

Figure 8 shows FE-SEM images of Ta irradiated by He plasma at high temperature, where (a) shows a typical small holes structure obtained at about 1300 K, while (b) was obtained by the process of an accidental temperature excursion from the above mentioned high temperature down to about 990 K. We can distinguish many tiny holes superposed on relatively large holes greater than 100 nm. It seems that shear modulus of Ta which characterizes viscous property could be too small to sustain any extension of nano-fibers. Shear modulus

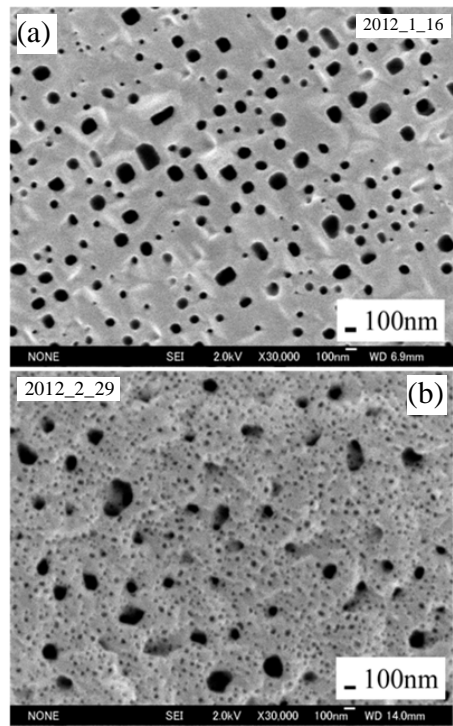


Fig.8 Helium defect of Ta target at relatively high temperature higher than about 1300 K. (a) Bubble formation with diameter of a few hundreds nm. (b) After temperature excursion from the high temperature down to 990 K. Tiny holes less than 100 nm with a very initial stage of loop formation.

of Ta is 69 GPa at room temperature, but it decreases with an increase in temperature so that the viscosity is not enough large at such a high temperature. This is also the case for W although the temperature range is quite different. At lower temperature range for Ta, some structure appear as shown in Fig.9 where the sample temperature was around 950 K and the He ion energy of 80 eV for more than four hours of He plasma irradiation. In (a) loop-like structure is seen on Ta sheet. The development depends on the grain. Figure 9(b) shows clearly loop-like structure formed on the surface with a large magnification. It seems that shear modulus would be still so small that a growth of fiber from loop-like structure could be difficult. At slightly lower temperature we do not obtain any morphological change. Therefore, we can say that the temperature band would be so narrow to have an appropriate shear modulus for a growth of nanostructure.

Precursor Identification and Physical Mechanism of Fiber-Form Nanostructure Growth on Metal Surfaces with Helium Plasma Irradiation

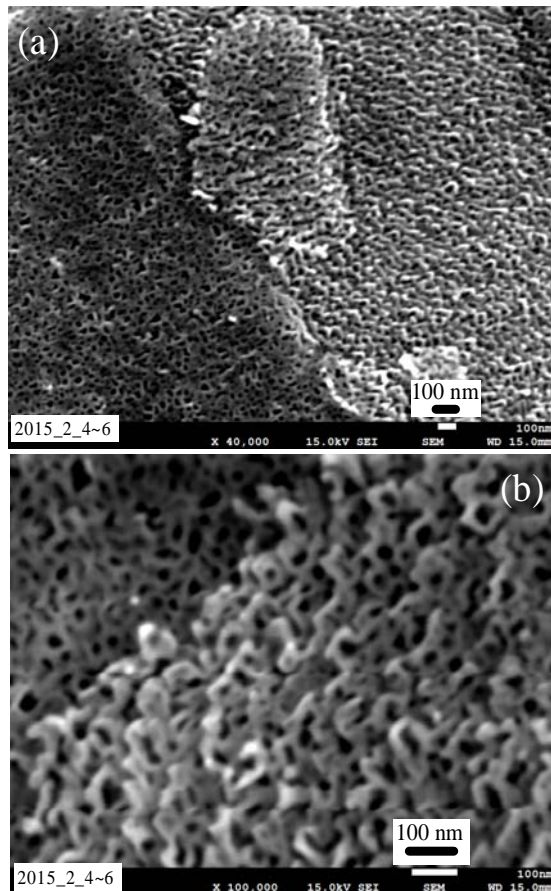


Fig.9 Helium defect of Ta target at intermediate temperature around 950 K (K-type thermocouple) with the He ion energy of 80 eV, the ion flux of  $1.2 \times 10^{21} \text{ m}^{-2} \cdot \text{s}^{-1}$  and the fluence of  $2.0 \times 10^{25} \text{ m}^{-2}$ . (a) Loop-like structure on Ta sheet and a grain boundary, and (b) Loop-like nanostructure formed on the surface with a magnified view.

#### 4. Discussions

##### 4.1 Modeling

From the above-mentioned observations, it is thought that loop-like structure is a kind of precursor for a growth of nano-fibers especially for W and Mo. Currently, it is not clear how nano-fibers are developed from such loop-like structures. Possible mechanisms include loop fracture due to bursting of bubbles containing He gas with a high pressure or branching growth from loops, that is a kind of bifurcation. Some physical properties ensuring the growth of nano-fibers will be discussed in the next subsection.

We summarize the experimentally observed growth process phenomenologically by using Fig.10<sup>24)</sup>. This

was accomplished by the flux-gradient method which converts time variations of fiber-form nanostructure growth in a single He plasma exposure of metals to spatial variation in metal surfaces.

(1)~(4): A pitting of a original base surface, resulting from hole formation. Bubbles inside the bulk migrate thermally near the surface and burst to release He gas.

(5)~(6): The hole area becomes large as He ion fluence increases so that a fine-grained miniaturization of the surface proceeds, making a kind of nano-walls, which may become a background of a precursor formation. The nano-wall contains also nano-bubbles inside which makes a hole near its center passing through the wall, resulting in a loop structure.

(7)~(8): Before growth of nano-fibers, randomly oriented, loop-like structures appear as a precursor growing to nano-fibers. The loop size increases as He ion fluence increases because of a possible surface tension exerted by the nano-bubbles inside.

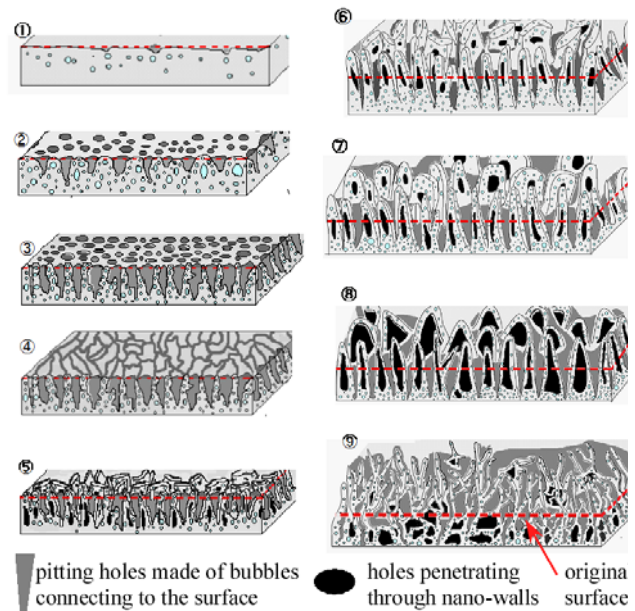


Fig.10 Modeling of nano-fiber growth on metal surfaces from bubble-made holes formation through loop-like structures finally to nano-fiber formation.

##### 4.2 Relation to Physical Properties of Metals

Here, possible relations of nanostructure growth to physical properties of materials are discussed. Table I is a summary from this view point. As suggested in the

Table 1 Physical properties of materials and relation to nanostructure growth

Z	Material	Crystal Structure	Melting Point [K]	Shear Modulus [GPa]	Nanostructure Growth
74	Tungsten (W)	bcc	3695	161	○ <sup>1)</sup>
75	Rhenium (Re)	hcp	3459	178	?
42	Molybdenum (Mo)	bcc	2896	126	○ <sup>10)</sup>
73	Tantalum (Ta)	bcc	3290	69	△
28	Nickel (Ni)	fcc	1728	76	○
26	Iron (Fe)	bcc, fcc	1811	82	○ <sup>26)</sup>
22	Titanium (Ti)	hcp	1941	41~44	□ <sup>26)</sup>
14	Silicon (Si)	diamond cubic	1687	51~80 <sup>27)</sup>	?

first section, the nanostructure growth seems very much related to shear motion of concerned materials. Shear flow in viscoelastic model is represented in terms of viscosity, while shear motion in solid materials is described in terms of shear modulus. The values for some solid materials are shown in Table I where other physical properties, such as melting point and crystal structure, are also shown in relation to nanostructure growth. W and Mo has a large shear modulus greater than 100 GPa at room temperature so that Rhenium having a large shear modulus has a chance to have a similar fiber-form nanostructure. Ni has a fairly low value of 76 GPa, while Ta has 69 GPa, further lower value. We speculate that these figures would be close to critical value for sustaining a continuous growth of nano-fibers. Below this value, a strain would be too small to support a nanostructure growth, and the structure would shrink rather than grow, which we may imagine a soft syrup. That is the reason why Ta shows a loop-like precursor nanostructure but not a development of nano-fibers. The temperature band would be so narrow that it could not continue to sustain a growth over a vertical range perpendicular to the original surface.

We have to note, firstly that the shear modulus is decreasing as the temperature increases<sup>15),25)</sup> and secondly that it is influenced by the presence of He clusters or nano-bubbles<sup>6)</sup>.

Titanium (Ti) has a further low value of shear modulus while it has two kinds of nanostructure<sup>26)</sup>. One structure, however, is cone-like at lower temperature and another is similar to fiber-form at higher temperature. Therefore, we cannot definitively say that the shear modulus at room temperature without He

atoms, clusters or bubbles is a unique measure for the nanostructure growth. We have to take into account its temperature dependences and effects of He clusters and bubbles. Moreover, mobilities of He atoms, clusters and bubbles should be ensured, which make a lowest temperature limit.

At the moment, crystal structure seems not to be an important parameter although shear modulus has a dependence of crystal orientation as shown in the case of silicon. Therefore, some difference would appear among grains for poly-crystal materials as shown in Fig.9(a).

## 5. Summary and Conclusions

Growth mechanism of fiber-form nanostructure on metal surfaces has been speculated by FE-SEM observations with a special technique that allows one to observe time evolutions of fiber-form nanostructure growth in a single He plasma exposure of metals. We call this technique flux gradient method which is obtained simply with a partial covering of metal surfaces.

The modeling based on experimental observations shows a pitting of the original base surface, resulting from bubbles formation in the bulk. The nano walls with a hole near the center develop as loop or arch like structure. The wall stands almost perpendicular to the surface, but the orientation seems to be random. The loops become large with an increase in He ion fluence. A development from loops to arborescent fibers may be caused by branching or fracturing due to bursting of He bubbles.

It is very difficult but curious question what physical

Precursor Identification and Physical Mechanism of Fiber-Form Nanostructure Growth on  
Metal Surfaces with Helium Plasma Irradiation

property of materials determines the growth of fiber-form nanostructure. The authors claim a magnitude of shear modulus of materials which is influenced by both temperature and He content. A very appropriate range of values for shear modulus which is able to sustain a growth of nano-fibers would exist. If the temperature band which satisfies the above requirement is enough large and ensure mobilities of He atoms, clusters and bubbles in the bulk, loops and fibers, then nano-fibers are able to grow. If such a temperature band is so narrow and/or does not ensure any mobility of He, then nano-fibers are not available although bubbles and holes are created at high temperatures.

Ta seems to be at a specific position from the above criterion. The shear modulus of Ta at room temperature without He content is larger than the value of Ti which gives a cone-like nanostructure at low temperature, somewhat different from other structure such as W, Mo, Fe and Ni, as well as fiber-form nanostructure at relatively high temperature. In the case of Ti, loop-like structure seems to be a precursor for nanostructure formation only at high temperature. Well-developed nanostructure of Ni is also unique.

As shown in Table I, it is quite interesting to investigate other materials including nonmetals as a reference of shear modulus<sup>27)</sup>.

### Acknowledgement

The work was supported by Grant-in-Aid for Scientific Research 26420855 from JSPS. One of the authors (S. Takamura) would like to thank Dr. A. Ito of NIFS, Prof. N. Ohno and Dr. S. Kajita of Nagoya University, and Prof. Y. Ueda of Osaka University for the basic discussions and Mr. T. Kobayashi of Yumex Inc. for his assistance on FE-SEM observations.

### References

- 1) S. Takamuran, N. Ohno, D. Nishijima and S. Kajita : "Formation of Nanostructured Tungsten with Arborescent Shape due to Helium Plasma Irradiation", Plasma Fusion Res. Vol.1, pp.051(2 pages), 2006.
- 2) M.I. Baldwin and D.P. Doerner : "Helium induced nanoscopic morphology on tungsten under fusion relevant conditions", Nucl. Fusion Vol.48, pp.035001(5 pages), 2008.
- 3) 高村秀一、梶田信、大野哲靖：「ヘリウムプラズマ照射により高融点金属表面に形成されたナノ構造」, 日本物理学会誌, Vol.68, No.9, pp.602-611, 2013.
- 4) S. Kajita, N. Yoshida, R. Yoshihara, N. Ohno and M. Yamagiwa : "TEM observation of the growth process of helium nanobubbles on tungsten : Nanostructure formation mechanism", J. Nucl. Mater., Vol.418, pp.152-158, 2011.
- 5) S.I. Krasheninnikov, "Viscoelastic model of tungsten 'fuzz' growth", Phys. Scr. Vol.T145, pp.014040 (4 pages), 2011.
- 6) R.D. Smirnov and S.I. Krasheninnikov : "On the shear strength of tungsten nano-structure with embedded helium", Nucl. Fusion Vol.53, pp.082002(4 pages), 2013.
- 7) F. Sefta, K.D. Hammond, N. Jaslin and B.D. Wirth : "Tungsten surface evolution by helium bubble nucleation, growth and rupture", Nucl. Fusion Vol.53, pp.073015 (pages), 2013.
- 8) Yu.V. Martynenko and M.Yu. Nagel : "Model of Fuzz Formation on a Tungsten Surface", Plasma Physics Reports Vol.38, No.12, pp.996-999, 2012.
- 9) G.M. Wright, D. Brunner, M.I. Baldwin, R.P. Doerner, B. Labombard, B. Lipschultz, J.L. Terry and D.G. Whyte : Nucl. Fusion Vol.52, pp.042003 (pages), 2012.
- 10) S. Takamura : "Temperature Range for Fiber-Form Nanostructure Growth on Molybdenum Surfaces due to Helium Plasma Irradiation", Plasma Fusion Res. Vol.9, pp.1405131 (4pages), 2014.
- 11) S. Kajita, T. Saeki, Y. Hirahata and N. Ohno : "Formation of Metallic Nanostructure by Helium Plasma Irradiation", Jpn. J. Appl. Phys. Vol.50, pp.01AH02(4 pages), 2011.
- 12) T. Miyamoto, S. Takamura and H. Kurishita : "Recovery of Tungsten Surface with Fiber-Form Nanostructure by Plasma Exposure", Plasma Sci. Technol. Vol.15, No.2, pp.161-165, 2013.
- 13) K.B. Woller, D.G. Whyte and G.M. Wright : "Dynamic measurement of the helium content of evolving tungsten nanostructures using Elastic Recoil Detection during plasma exposure", 21<sup>st</sup> International Conf. on Plasma Surface Interactions in Controlled Fusion Devices, Kanazawa, P1-001, Japan, 26-30 May, 2014.
- 14) S. Takamura : "Characteristics of the Compact Plasma Device AIT-PID with Multicusp Magnetic Configuration", IEEJ Trans. E. E. Eng. Vol.7(S1), pp.S19-S24, 2012.
- 15) E. Lassner and W.-D. Schubert : "Tungsten", Kluwer Academic / Plenum Publishers, New York, 1999.

- 16) M.Y. Ye, S. Takamura and N. Ohno : "Study of hot tungsten emissive plate in high heat flux plasma on NAGDIS-I", J. Nucl. Mater. Vol.241-243, pp.1243-1247, 1997.
- 17) D. Nishijima, M.Y. Ye, N. Ohno and S. Takamura : "Formation mechanism of bubbles and holes on tungsten surface with low-energy and high flux plasma irradiation in NAGDIS-II", J. Nucl. Mater. Vol.329-333, pp.1029-1033, 2004.
- 18) H. Illmaier : "The influence of helium on the bulk properties of fusion reactor structure material", Nucl. Fusion Vol.24, pp.1039-1084, 1984.
- 19) A.M. Ito et al. : "Molecular dynamics research on formation mechanism of tungsten nanostructure induced by helium plasma irradiation", 21<sup>st</sup> International Conf. on Plasma Surface Interactions in Controlled Fusion Devices, I14, Kanazawa, Japan, 26-30 May, 2014.
- 20) W. Sakaguchi, S. Kajita, N. Ohno and M. Takagi : "In situ reflectivity of tungsten mirrors under helium plasma exposure", J. Nucl. Mater. Vol.390-391, pp.1149-11523, 2009.
- 21) S. Takamura : "Initial Stage of Fiber-Form Nanostructure Growth on Refractory Metal Surfaces with Helium Plasma Irradiation", Plasma Fusion Res. Vol.9, pp.1302007 (3pages), 2014.
- 22) S. Takamura : "Power Transmission Factor through the Sheath in Deuterium Plasmas for Virgin as well as Nanostructured Tungsten", 21<sup>st</sup> International Conf. on Plasma Surface Interactions in Controlled Fusion Devices, P3-002, Kanazawa, Japan, 26-30 May, 2014.
- 23) S. Sharafat, A. Takahashi, K. Nagasawa and N. Ghoniem : "A description of stress driven bubble growth of helium implanted tungsten", J. Nucl. Mater. Vol.389, pp.203-212, 2009.
- 24) 高村秀一：「高融点金属表面に成長する繊維状ナノ構造形成初期段階に関する実験的考察」プラズマ研究会資料 (The paper of technical Meeting on Plasma Science and Technology, IEE Japan, PST-14-43)、電気学会、2014年9月9日。
- 25) R. Farraro and R.B. McLellan, "Temperature dependence of the Young's modulus and shear modulus of pure nickel, platinum, and molybdenum", Trans. A, Vol.8A, pp.1563-1566, 1977.
- 26) S. Kajita, T. Yoshida, D. Kitaoka, R. Etoh et al.: "Helium plasma implantation on metals: Nanostructure formation and visible light photocatalytic response", J. Appl. Phys. Vol.113, p.134301(7 pages), 2013.
- 27) M.A. Hopcroft, W.D. Nix and T.W. Kennt, "What is the Young's Modulus of Silicon?", J. Microelectromech. Syst. Vol.19, pp.229-238, 2013.

(受理 平成 27 年 3 月 19 日)